

Dark Matter and Metal Abundances in Elliptical Galaxies from X-ray Observations of the Hot ISM

Michael Loewenstein

NASA/GSFC, Code 662, Greenbelt, MD 20770, USA

Abstract. I review the results of recent analysis and interpretation of X-ray observations of elliptical galaxies, focusing on elemental abundances and dark matter. The hot ISM is characterized by subsolar Fe abundances and solar Si-to-Fe ratios; and, I compare these with stellar abundances and discuss implications of these measurements. From models constructed to explain X-ray temperatures and their correlation with optical properties in a complete sample of ellipticals, I demonstrate the ubiquity of dark matter in $L > L_*$ galaxies, present limits on dark matter structural parameters, and discuss the scaling of dark halos with optical luminosity. The mass-to-light ratio within $6R_e$ has a universal value, $M/L_V \approx 25h_{80}M_\odot/L_{V_\odot}$, that conflicts with the simplest extension of CDM theories of large scale structure formation to galactic scales.

1. Introduction and Overview

In this contribution I review the properties of the hot, X-ray emitting gas in elliptical galaxies. The investigation of elliptical galaxies using X-ray observations is a less mature and more volatile field than its radio and optical counterparts; however, X-ray studies provide unique and complementary insights into the nature of these systems. I concentrate on two topics of relevance to the subject of this conference, star formation in early-type galaxies.

The first topic is the nature of the X-ray emission, focusing on the hot gas metallicity. The mass, distribution, and relative abundances of metals constrain the enrichment and, therefore, the star formation history of these galaxies. The complicated nature of optical abundance studies emphasizes the value of the complementary method of X-ray spectroscopy of hot gas that originates as stellar mass loss. In this portion of the review, I explain and evaluate the “standard” model for the X-ray emission from elliptical galaxies, and review the low abundances in elliptical galaxy hot interstellar media derived using such models. I also compare X-ray and optical abundances, summarize measurements of the Si-to-Fe ratio in the hot gas, and discuss some of the implications of the observed abundances. Many of the results I discuss here are based on the work of Kyoko Matsushita (Tokyo Metropolitan University), Hironori Matsumoto (Kyoto University) and, especially, Richard Mushotzky (NASA/GSFC).

The second part of this review is a summary of a recently completed project, in collaboration with Ray White (University of Alabama), on the existence and properties of dark matter halos in the population of bright elliptical galaxies.

Dark matter is a determining factor in the feedback processes that occur during the star formation epoch and are responsible for such correlations as the color-magnitude relation. I review our modeling methods and assumptions and summarize the following results: (a) a demonstration of the ubiquitousness of dark matter in ellipticals, (b) how the dark halo properties must scale with optical properties to match the observed X-ray/optical correlations, and (c) implications for galaxy formation and cosmology.

2. X-ray Emission from Elliptical Galaxies – General Considerations

Surprisingly – since it was expected that galactic winds would drive out most gas (Mathews & Baker 1971) – the *Einstein* Observatory discovered that many elliptical galaxies are bright in X-rays, with luminosities up to $\sim 10^{42}$ erg s $^{-1}$ (Fabbiano 1989). The X-ray luminosity is a steep function of optical luminosity ($L_X \propto L_{opt}^{2.5}$), and X-ray studies are highly biased towards the optically brightest systems, many of which are in the Virgo cluster.

In the brightest systems, the emission is dominated by $\sim 10^7$ K gas, and the gas mass within the optical galaxy can be as high as a few percent that of the stars – much less than the stellar mass loss rate integrated over a Hubble time. The gross properties of the hot gas are well explained by hydrodynamical models where gas is heated by stellar motion-induced shocks and (possibly) Type Ia supernovae (SNIa), and settles into hydrostatic equilibrium in a gravitational potential that includes dark matter (Loewenstein & Mathews 1987).

Some elliptical galaxies have very extended (> 100 kpc in radius) X-ray coronae. This is not surprising – a galaxy of 10^{11} L $_{\odot}$, stellar $M/L = 10$, and baryon fraction 5% has a viral radius ~ 500 kpc. It is not clear whether the gas in these extended halos represents a primordial baryon reservoir or was ejected from the galaxy during an early star forming epoch, nor is it understood why other galaxies have compact X-ray halos.

The study of the X-ray emission from elliptical galaxies has greatly intensified this decade due to the superior spectral and imaging capabilities of the *ROSAT* and *ASCA* observatories. This has led to tremendous improvements in the accuracy and extent of derived gas density and temperature profiles, as well as the first significant sample of accurate gas abundances. These new observations are the foundation of the insights into elliptical galaxy structure and evolution that I now discuss.

3. The “Standard” Model

ASCA spectra can generally be decomposed into soft and hard components (Matsumoto *et al.* 1997, Matsushita 1997). The soft component originates in the hot (0.3–1.2 10^7 K) ISM, and shows a wide range of X-ray-to-optical flux ratios and X-ray extents for any optical luminosity. The hard component is roughly co-spatial with the optical galaxy, and scales linearly with optical luminosity with a relative normalization and spectrum consistent with measurements of the integrated emission from low mass X-ray binaries in spiral galaxy bulges (although some galaxies appear to have enhanced hard emission from a spatially unresolved nucleus). I will refer to this two-component model as the “standard”

model, since it is the simplest model that describes the data. Since abundance uncertainties become large as the hard component begins to dominate and emission line equivalent widths are diluted, accurate abundances are derivable only in gas-rich ellipticals, of which there are about 20 in the *ASCA* archive. This includes galaxies with both extended and compact X-ray morphologies.

4. Hot Gas Abundances in the Standard Model

Figure 1 shows a plot of abundance versus temperature derived from *ASCA* spectra extracted from the inner $5R_e$ using the standard model. The soft component is modeled using the Raymond-Smith thermal plasma emission code with abundances fixed at their solar photospheric ratios (abundance of Fe relative to H 4.68 10^{-5} by number). The abundances – essentially the Fe abundance as X-ray spectra at these temperatures are dominated by Fe L emission lines – range from about 0.1 to 0.7 solar. Since it is usually assumed that abundances of the mass-losing stars that are the origin of the hot gas are supersolar, these may seem surprisingly low. Moreover, Type Ia supernovae exploding at a rate R_{SNIa} SNU (1 SNU = 1 SN per 10^{10} L_{B_\odot} per 100 yr) should further enrich the hot gas by an additional $\sim 25R_{SNIa}$ solar – or ~ 2.5 times solar using the rate from Cappellaro et al. (1997) for $H_0 = 65$ km s $^{-1}$ Mpc $^{-1}$. Thus, X-ray abundances of elliptical galaxies are > 5 times less than what might naively be expected.

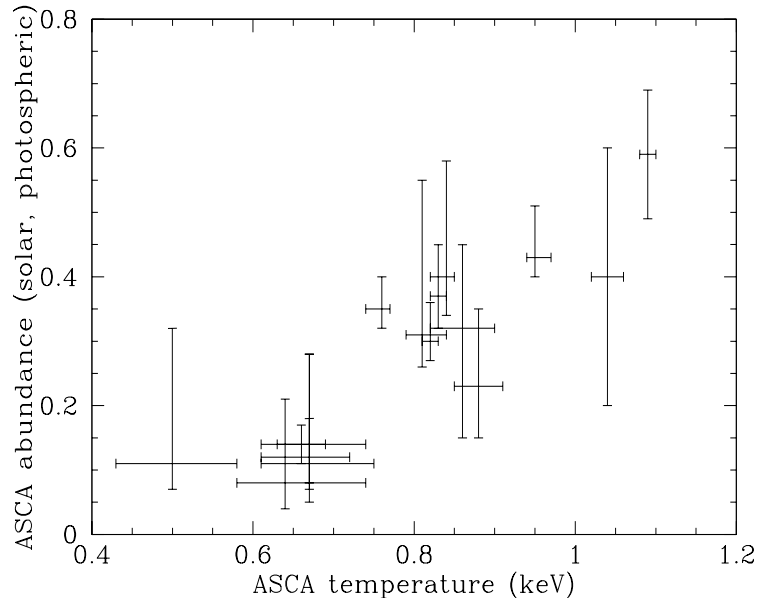


Figure 1. Hot gas metal abundance, assuming solar photospheric ratios, versus temperature – mostly adapted from Matsushita (1997).

5. X-ray/Optical Metallicity Comparison Revisited

5.1. X-ray Advantages and Disadvantages

Physical quantities such as hot gas abundances and temperatures are derived from model fitting of X-ray spectra. For abundance studies, a great advantage of X-ray spectroscopy is that – given sufficient signal-to-noise, spectral resolution, bandpass, and knowledge of the the important atomic transitions – emission line strengths provide *direct* measurements of elemental abundances. This is not the case for optical abundances (“the intensity of Mg_2 does not simply correlate with the abundance of Mg”; Tantalo, Bressan, & Chiosi 1998).

ASCA has those qualities required for abundance determinations of the X-ray brightest elliptical galaxies. However, there are limitations. The bandpass and energy resolution are insufficient to obtain clean measurements of many elements; the atomic parameters for some of the prominent Fe emission features are uncertain; spectra can be complicated by multiple components not spatially separable due to the limited *ASCA* angular resolution. “Contamination” by SNIa explosions or accretion of intergalactic gas may complicate the comparison with stellar abundances. However the low measured hot gas Fe measurements argues against the former, while the lack of an anti-correlation between hot gas metallicity and X-ray luminosity apparently rules out the latter.

One can obtain fairly accurate Fe abundances for 20 or so galaxies, Si abundances for about half that number, and occasionally some constraints on O, Mg, and S. A comparison with the optical results seems to be meaningful if we focus on the X-ray emission from the optical region of the galaxy.

5.2. Is There Evidence of an X-ray/Optical Discrepancy?

Measurements of the nuclear Mg_2 index imply that elliptical galaxies have supersolar abundances only if one assumes (a) that metallicities are constant with radius, (b) that abundances have solar ratios, and (c) that all stars were formed a Hubble time ago. For a meaningful comparison with the X-ray abundances, one needs to estimate a globally averaged stellar Fe abundance. Negative abundance gradients indicate that the average metallicity is typically a factor of two below the central value (Arimoto et al. 1997), and Fe is underabundant, typically by an additional factor of two, relative to Mg (Worley, Faber, & Gonzalez 1992). These factors bring the optical and X-ray Fe abundances into fair agreement. This is illustrated by the *ASCA* Fe abundance profile for NGC 4636 (Mushotzky et al. 1994, Matsushita et al. 1998) shown in Figure 2, where a comparison is made with the extrapolated optical Mg_2 profile (Davies, Sadler, & Peletier 1993) converted to [Fe/H] assuming three separate values of [Mg/Fe] (Matteucci, Ponzone, & Gibson 1998). There is no clear discrepancy once the effects of gradients and non-solar abundance ratios are properly accounted for.

Additional complications have emerged from recent work in this field. Balmer emission line measurements indicate that many elliptical galaxies have undergone star formation relatively recently, compromising the simple conversion from a single line index to metallicity. Scott Trager has kindly provided me with *very preliminary* estimates, based on work underway in collaboration with J. Gonzalez, S. Faber, and D. Burstein that accounts for the effects of differences in stellar population and non-solar abundance ratios, of the Fe abundance at the half-light

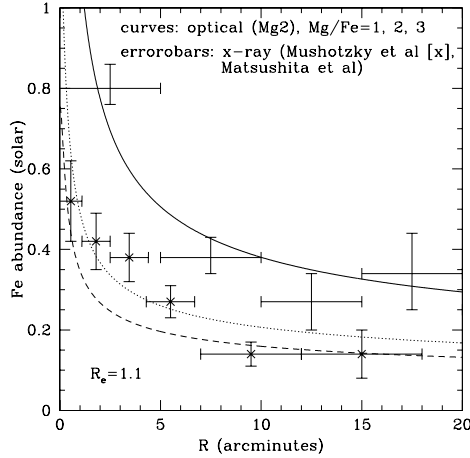


Figure 2. Hot ISM Fe abundance compared with the extrapolated optical estimates with $Mg/Fe = 1$ (solid curve), 2 (dotted curve), and 3 (dashed curve) times solar.

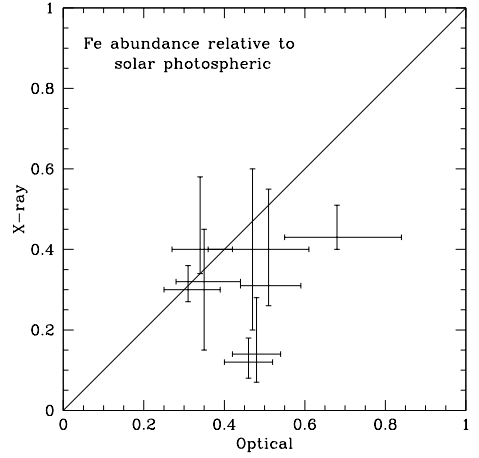


Figure 3. X-ray versus optical global Fe abundance.

radius (R_e) that I have converted to a global average. There is an overlap of eight galaxies with the gas-rich *ASCA* sample; and, there is generally a rough consistency (Figure 3). The (unweighted) average optical Fe abundance is ~ 0.45 solar compared to ~ 0.3 solar for the hot gas, with the offset dominated by two extreme gas-underabundant systems. The “optical/X-ray abundance discrepancy” is primarily an artifact of abundance gradients and non-solar abundance ratios, greatly diminished once the proper comparison – of average measurements of the same element over the same aperture – is made.

5.3. Is the Standard Model Correct?

The fair consistency of optical and X-ray abundance determinations mitigates one of the primary objections to the adequacy of the simple two-component “standard” model. Inaccuracies in our knowledge of Fe L atomic physics (Arimoto et al. 1997), has been shown to be no more than a 20–30% effect (Hwang et al. 1997, Buote and Fabian 1998a).

A more formidable alternative to the standard model has been constructed by Buote and Fabian (1998b). They found that the best fit to *ASCA* data often consists of a two-temperature plasma, with the secondary component having a temperature of 1.5–2 keV, and that the abundances in such fits are systematically higher by about a factor of two compared to the standard model. However, we have found that He-like to H-like Si line ratios are in precise agreement with the predictions of the standard model (Figure 4; Mushotzky & Loewenstein 1998), although *ASCA* spectra are not of sufficient quality to generally and unambiguously rule out the Buote and Fabian two-phase model.

A final argument for the correctness of the standard model comes from the demonstration that, in NGC 4649 and NGC 4472, the mass profile obtained from the hot gas temperature in single phase fits is in perfect accord with the mass determined optically (Brighenti & Mathews 1997).

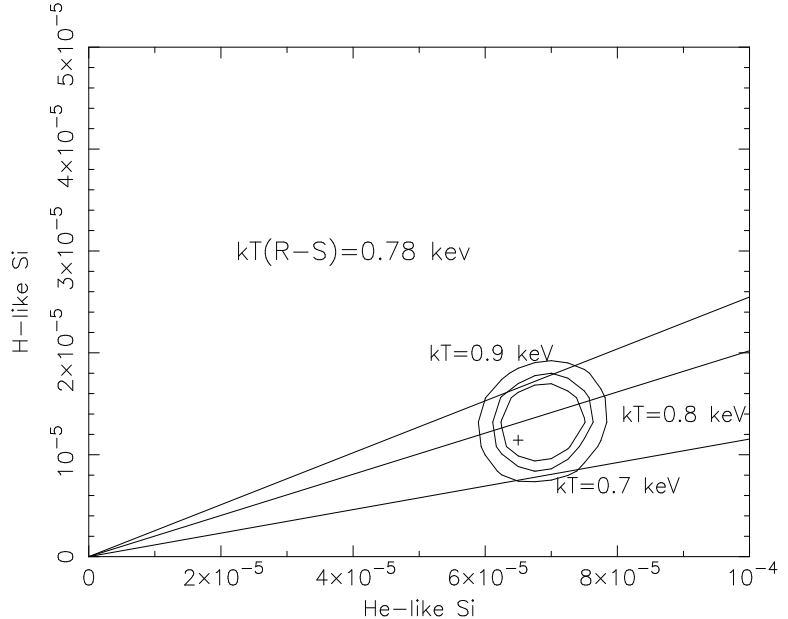


Figure 4. 68, 90, and 99% confidence contours for H- and He-like Si line strengths (in photons $\text{cm}^{-2} \text{s}^{-1}$) in the elliptical galaxy NGC 4636. The solid lines show the ratios expected in three single-temperature thermal plasma models. The temperature derived from global spectral fitting is in precise agreement with the line diagnostic value.

6. Si-to-Fe Ratio in the Hot Gas

Elemental abundance ratios provide constraints on the primordial IMF and relative numbers of Type Ia and Type II supernovae. Renormalized to the meteoritic Fe abundance, the Si-to-Fe ratio lies between 0.5 and 1.5 times solar (Figure 5). This is lower than the Mg-to-Fe ratio derived from nuclear optical spectra, and is more in line with values measured from the X-ray spectra of intragroup media. This implies that either the α -to-Fe enhancement is a phenomenon restricted to the inner ($< R_e$) galaxy, or that the Si-to-Mg ratio is subsolar. Evidently, intracluster media (Loewenstein & Mushotzky 1996) and elliptical galaxy cores have the enhanced α -to-Fe elemental ratios characteristic of rapid high mass star formation where enrichment is dominated by Type II supernovae, while groups and the outer regions of elliptical galaxies tend toward the solar supernovae mix where a larger fraction of Fe originates in SNIa.

The Si abundance provides a robust upper limit on the effective SNIa rate that is consistent with that derived using Fe. The conservative (assuming that

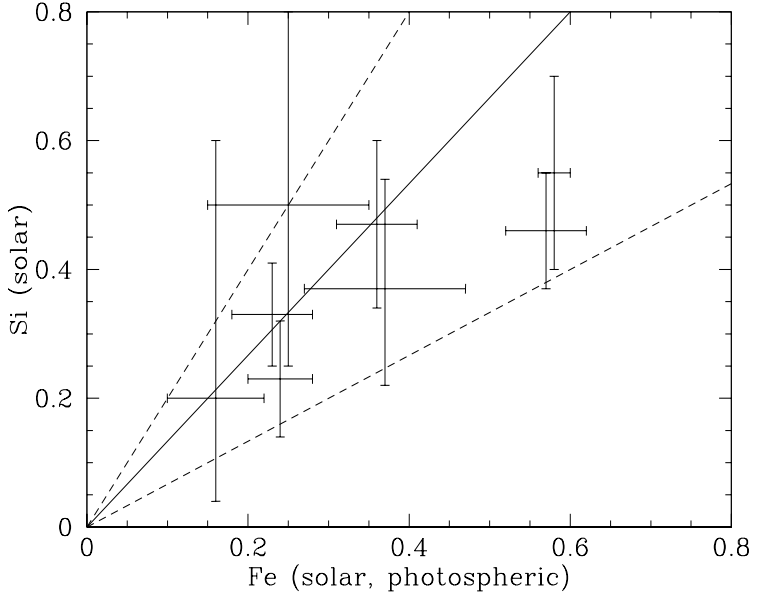


Figure 5. Si versus Fe abundance in the hot X-ray emitting gas. The solid line denotes Si:Fe in the ratio 1:1, while the broken lines denote the ratios 3:2 and 1:2 with respect to the (meteoritic) solar ratio.

all of the Si in the hot gas originates from SNIa) limit is typically ~ 0.03 SNU – about four times lower than the recent estimate of Cappellaro *et al.* (1997).

7. Implications of Low Abundances

A globally averaged Fe abundance in elliptical galaxies of about half-solar is in accord with optical and X-ray spectroscopic measurements, as well as with predictions of chemically consistent evolutionary models (Möller, Fritze-v. Alvensleben, & Fricke 1997). As this is only slightly higher than the ICM Fe abundance, and the ICM dominates the cluster baryon mass, there is considerably more Fe in the ICM than is locked up in cluster galaxy stars. This implies one of the following.

(1) If the stellar and ICM metals come from the same SNII-enriched proto-elliptical galaxy gas, then 50–90% of the original galaxy mass was lost and much of the ICM is not primordial but was ejected from galaxies. (2) However, the actual mass of material directly associated with the SNII ejecta is much less significant. Selective mass-loss of nearly pure SNII ejecta would enable expulsion of much of the metals while retaining most of the baryonic mass. There is both observational (Kobulnicky & Skillman 1997) and theoretical (Mac Low & Ferrara 1998) evidence for super-enriched outflows in dwarf galaxies that may serve as analogues of pre-merger elliptical galaxy sub-units.

(3) It is possible that the ICM enrichment originates in some other source. The most plausible candidates are dwarf galaxies, but Gibson & Matteucci

(1997) have shown that this scenario is not consistent with the color-magnitude relation in these systems. Therefore, one may have to appeal to a population of dwarf galaxies that destroy themselves in the process of enriching the ICM.

Models of the chemical evolution of elliptical galaxies are often tuned to produce supersolar stellar abundances, reproduce the color-magnitude diagram, explain ICM enrichment, etc. They also tend to predict high ISM metallicities (e.g., Matteucci & Gibson 1995). Re-evaluation of these models in light of the downward revision of elliptical galaxy metallicities may be in order.

8. Dark Matter in Elliptical Galaxies: Background and Motivation

I now turn to the second main topic of this review, dark matter in elliptical galaxies. There is a strong consensus that dark matter dominates the mass content of spiral galaxies, galaxy groups and clusters, and the universe as a whole. Although traditionally less forthcoming and more controversial, evidence for dark matter in elliptical galaxies has rapidly accumulated in recent years from improved stellar dynamical data and modeling, gravitational lensing observations, and high-quality X-ray images and spectra from the *ROSAT* and *ASCA* satellites. For example, the extended flat hot gas temperature profiles measured using *ASCA* (Matsushita 1997) are analogous to flat HI rotation curves in spiral galaxies as indicators of the presence of massive dark matter halos.

Although the case for dark matter in some ellipticals is now overwhelmingly strong, we (Loewenstein & White 1998) were motivated by published measurements of X-ray temperatures in a complete optically selected sample (Davis & White 1996), to attempt to answer the following more general questions: (1) Do bright elliptical galaxies have dark matter halos *in general*? (2) How do the dark halo properties scale with optical luminosity?

9. Modeling and Assumptions

The primary diagnostic observable in this work is the ratio of stellar to hot gas temperatures, $\beta_{\text{spec}} \equiv \mu m_p \sigma^2 / k \langle T \rangle$, where μm_p is the mean mass per particle, σ the projected central optical velocity dispersion, and $\langle T \rangle$ the globally (*i.e.*, over $6R_e$) averaged gas temperature. From the fundamental plane relations and virial theorem for the the gas, it follows that β_{spec} is an excellent diagnostic of the total mass-to-light ratio. The following characterize the “ T – σ ” relation, and must be reproduced by any successful model of the dark matter in elliptical galaxies: (1) $\beta_{\text{spec}} < 1$ (the gas is always hotter than the stars, typically by factors of 1.5–2), and (2) $\langle T \rangle \propto \sigma^{1.45}$ or $\beta_{\text{spec}} \propto \sigma^{0.55}$ (Davis & White 1996).

(1) Stars and gas are assumed to be in hydrostatic equilibrium in a spherically symmetric gravitational potential. (2) Stellar orbits are assumed to vary monotonically from isotropic at the center to radial at infinity. (3) Stellar density profiles and scaling relations are determined by *HST* observations (Faber et al. 1997) and the fundamental plane. (4) The “NFW” dark-matter parameterization (Navarro, Frenk, & White 1997) is adopted,

$$\rho_{\text{dm}}(r) \propto \left(\frac{r}{R_{\text{dm}}} \right)^{-1} \left(1 + \frac{r}{R_{\text{dm}}} \right)^{-2}, \quad (1)$$

where ρ_{dm} and R_{dm} are the dark matter density distribution and scale length, respectively. β_{spec} is primarily determined by the dark-to-luminous mass ratio inside the optical radius (R_{opt} , defined here as $6R_e$, the radius enclosing $\approx 90\%$ of the light), and the dark halo concentration (the ratio of dark matter to stellar scale lengths). A global observable, β_{spec} is not sensitive to the functional form of the dark matter density distribution; the choice of equation (1) enables us to connect our results with numerical structure formation simulations.

10. Dark Matter Universality and Limits

$\beta_{\text{spec}} > 1.2$ for models without dark matter — greater than in any observed galaxy (Davis & White 1996). A typical value of $\beta_{\text{spec}} = 0.5$ requires a dark-matter fraction of $\approx 75\%$ within R_{opt} for $R_{\text{dm}} \approx R_e$. Although the dark matter distribution is not constrained in detail, more than half of the mass within R_e is baryonic for models with $\beta_{\text{spec}} = 0.5$ if $R_{\text{dm}} > R_e$. Even for extreme stellar models, β_{spec} *always exceeds* ≈ 0.75 *unless ellipticals have dark matter*. Therefore, dark halos must be generic to $L > L_*$ elliptical galaxies.

We place lower limits on the dark-matter scale length, R_{dm} — if the dark matter is too concentrated σ increases relative to $\langle T \rangle$, raising β_{spec} . The minimum value of R_{dm} consistent with $\beta_{\text{spec}} \approx 0.5$ is $\approx 0.3R_e \approx 2(L_V/3L_*)^{3/4}h_{80}^{-1}$ kpc, where $L_* \approx 1.7 \times 10^{10}h_{80}^{-2}L_{V\odot}$ (Figure 6). We also derive upper limits on the baryon fraction, analogous to maximum disk models for spiral galaxies (Figure 7). The minimum dark matter mass fraction is $\approx 30\text{--}57\%$ within R_{opt} for $\beta_{\text{spec}} = 0.4\text{--}0.7$, and is $<20\%$ within R_e .

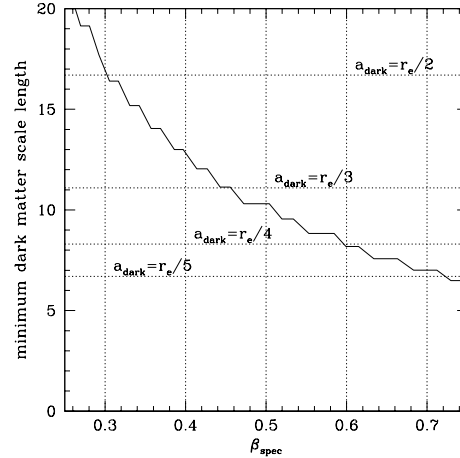


Figure 6. Minimum dark-matter scale length in units of the “break radius,” $0.03 R_e$.

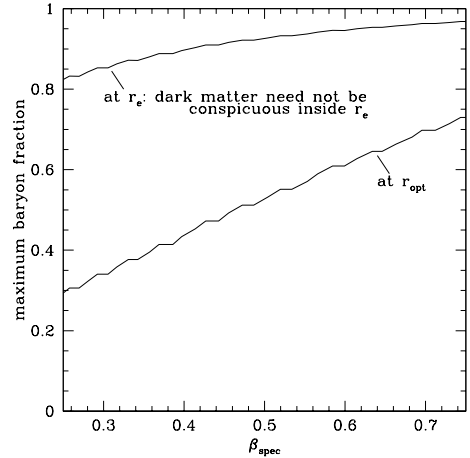


Figure 7. Maximum values of baryon fractions within R_e , and R_{opt} .

11. Explaining the $T-\sigma$ Relation

Elliptical galaxies with the same dark-to-luminous mass and scale length ratios have the same β_{spec} . As can be inferred from the virial theorem and fundamental plane relations, the observed trend wherein β_{spec} increases with increasing σ (or, equivalently, with L_V) implies that more luminous galaxies are *less* dark-matter dominated within R_{opt} (and in such a way that the total mass-to-light ratio is nearly constant). Extending our models to virial radius and mass scales, we investigate what dark matter scaling relations predict such a trend. Two successful scenarios are the following (Figure 8). (1) The dark matter scale length R_{dm} increases weakly with M_{virial} as predicted in CDM simulations, but the baryon fraction (f_{bar}) is an increasing function of optical luminosity, as expected if smaller galaxies undergo more intense supernova-driven mass loss during their star forming epoch (dotted curves in Figures 8, 9, and 10). If all ellipticals formed with the same f_{bar} , then the average $L > L_*$ galaxy has lost more than half its original mass. (2) All elliptical galaxies have the same f_{bar} but R_{dm} increases *much more steeply* with M_{virial} than in CDM models (dashed curves in Figures 8, 9, and 10). In this case, less luminous galaxies have relatively more dark matter within R_{opt} because of a more concentrated dark-matter distribution rather than a larger overall dark-matter fraction. This deviation from CDM predictions of dark halo scaling on mass scales $< 10^{14} M_{\odot}$ could result from a relatively flat primordial fluctuation spectrum or the effects on the dark matter density profile from evolution of the baryonic component.

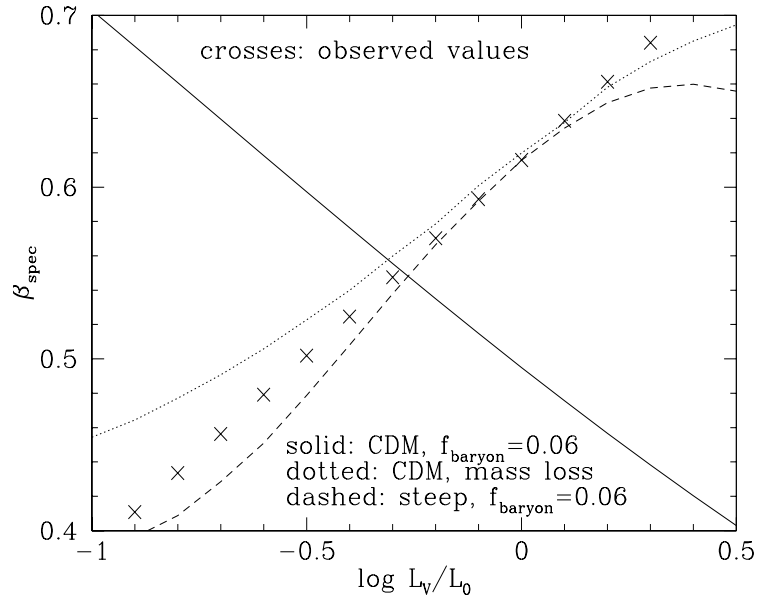


Figure 8. Observed and predicted correlation of β_{spec} with dimensionless luminosity ($L_o = 5.2 \times 10^{10} h_{80}^{-2} L_{V\odot}$). Solid curve denotes constant f_{bar} and CDM dark matter concentration scaling; dotted curve has f_{bar} increasing with luminosity; dashed curve has a steeper-than-CDM scaling of concentration with dark halo mass.

Models with dark halos that scale as predicted by CDM, but with constant f_{bar} , badly fail to reproduce the observed $T-\sigma$ trend (solid curve in Figure 8).

12. How Dark Matter Scales with Optical Luminosity

For the two scenarios described above that successfully reproduce the $T-\sigma$ relation, total masses within R_e and R_{opt} are perfectly consistent with gravitational lensing results (Griffiths et al. 1996; see Figure 9), as well as with those from studies of ionized gas disks as discussed by R. Morganti at this meeting. Integrated properties within R_{opt} are robust (Figure 10): $M/L_V \approx 25h_{80}M_{\odot}/L_{V\odot}$, ($f_{\text{bar}} \approx 0.35(L_V/3L_*)^{1/4}$). On scales both larger and smaller than R_{opt} , dark-matter scaling in the two scenarios described above diverges (Figures 9 and 10). In the constant f_{bar} , non-CDM scaling scenario, dark matter becomes increasingly important inside R_e as L_V decreases, becoming dominant for $L < 0.6L_*$.

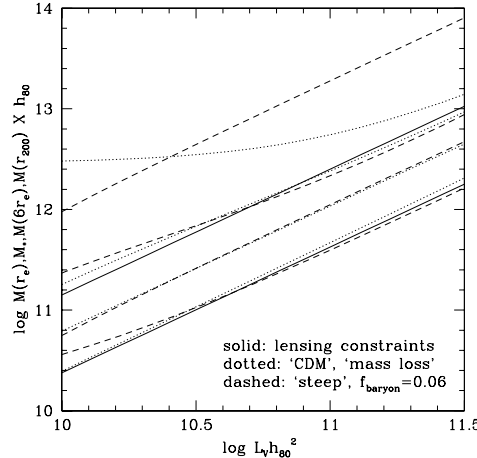


Figure 9. M vs L_V within (bottom to top) R_e , R_{opt} (stars), R_{opt} (total), and R_{virial} . Solid curves show $M(R_e)$ and $M(R_{\text{opt}})$ inferred from statistical weak lensing.

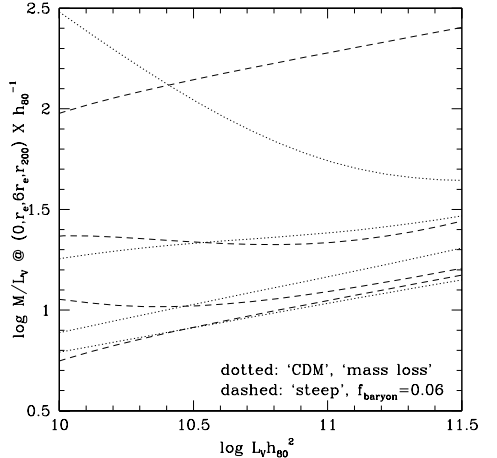


Figure 10. Same as Figure 9 for M/L_V at (bottom to top): $r = 0, R_e, R_{\text{opt}}, R_{\text{virial}}$.

We have calculated dark matter and stellar velocity dispersion distributions, assuming isotropic orbits. These are compared in Figure 11 for an $L_V = 5.2 \times 10^{10}h_{80}^{-2}L_{V\odot}$ galaxy for both of the successful scenarios described above and in Figures 9 and 10. Both distributions have maxima since the total gravitational potential is not isothermal. The ratio (dark-matter-to-stars) of the squares of these maxima is greater than 1.4 over the luminosity range in Figures 9 and 10, and is ≈ 2 over the range $L_* < L_V < 5L_*$. In fact, the minimum value of this ratio for any model that produces $\beta_{\text{spec}} < 0.7$ is greater than one. In this sense the dark matter is hotter than the stars, as simply reflected by the observation that the gas temperature exceeds that of the stars.

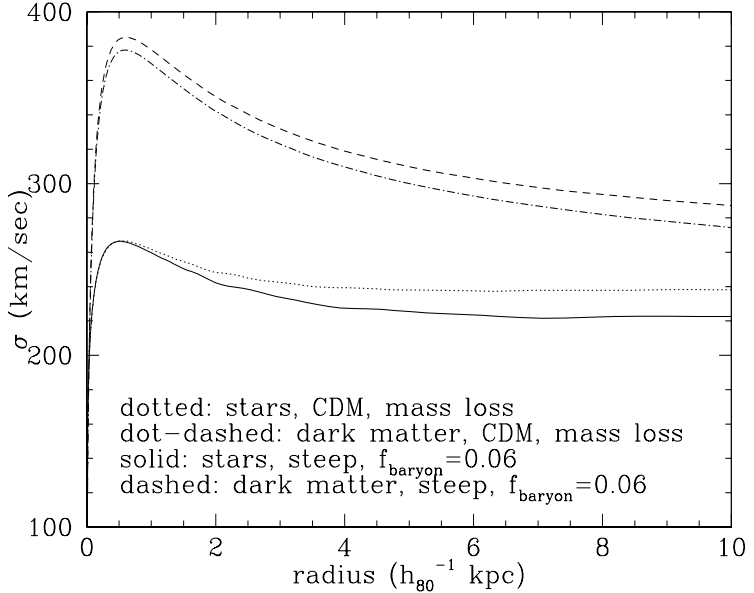


Figure 11. 1-d velocity dispersion distributions, assuming isotropic orbits, for an $L_V = L_0 = 5.2 \times 10^{10} h_{80}^{-2} L_{V_\odot}$ galaxy.

13. Summary

This review has focussed on two major investigations of the hot, X-ray emitting ISM in elliptical galaxies of relevance to the issue of star formation in elliptical galaxies – the nature and metallicity of the hot gas, and the properties of the dark matter halos confining the hot gas.

13.1. Abundances in the Hot ISM: Concluding Remarks

X-ray spectra of elliptical galaxies are adequately fit by models consisting of hot gas with subsolar Fe abundance and roughly solar Si-to-Fe ratio, plus a hard component from an ensemble of X-ray binaries. The consistency of the magnitude and spectrum of the hard component with that expected from X-ray binaries and its compact morphology, support this model over ones where the hard component is primarily due to a hotter gas phase. Complications in the form of an extra soft continuum or multiple phases can be considered, but the consistency of the Si line diagnostic and continuum temperatures demonstrates that the data – at the present level of sensitivity and spectral resolution – do not require these. Optical and X-ray Fe abundance estimates are converging, although there are some cases with anomalously low X-ray values.

Occam's razor would seem to demand that we provisionally accept the reality of low abundances in elliptical galaxies. As a result, we need to seriously reevaluate our notions of elliptical galaxy chemical evolution, intraccluster enrichment, and Type Ia supernova rates.

13.2. Dark Matter in Elliptical Galaxies: Main Conclusions

We (Loewenstein & White 1998) have constructed mass models of elliptical galaxies consistent with the fundamental plane scaling relations and *HST* results on the structure of the centers of elliptical galaxies, with dark halos as predicted by large scale structure formation simulations. These models allow us to calculate the diagnostic parameter β_{spec} as a function of the relative (to luminous) dark matter mass and scale length. Comparison with the observed mean $T-\sigma$ relation – the main features of which are that the X-ray emitting gas is always hotter than the stars, and by an amount that increases for galaxies of lower velocity dispersion/optical luminosity – provides constraints on the properties of dark halos around elliptical galaxies. Our main results are as follows.

(1) In the absence of dark matter, β_{spec} generally exceeds 1.2, with an absolute lower limit of 0.75. Since galaxies are observed to have $\beta_{\text{spec}} = 0.3\text{--}0.8$, we conclude that dark halos are generic to $L > L_*$ elliptical galaxies.

(2) The most natural explanation of the observed correlation of β_{spec} with luminosity is that less luminous galaxies are more dark-matter dominated inside R_{opt} in such a way that the total mass-to-light ratio is nearly constant. This ratio, $\approx 25h_{80}M_{\odot}/L_{V\odot}$, is exactly what is predicted for mass models of elliptical galaxies designed to explain the gravitational shear of background field galaxies measured for a disjoint sample of elliptical galaxies.

(3) Our models can be embedded within theories of large scale structure by specifying how the dark matter concentration scales with virial mass, and linking the virial mass to the observed luminosity by specifying a global baryon fraction. The standard CDM scaling with constant baryon fraction badly fails to reproduce the observed $T-\sigma$ relation, since it predicts an increase in dark-to-luminous ratio (inside R_{opt}) with luminosity. The following two successful variations are obtained by relaxing one of the two assumptions of the constant baryon fraction CDM scenario: (a) standard CDM scaling for the dark halos, but with smaller galaxies losing an increasingly large fraction of their initial baryonic content; or, (b) a constant baryon fraction, but with the dark-matter concentration varying much more strongly with virial mass than CDM models predict so that more luminous galaxies are less dark-matter dominated due to a relatively diffuse (rather than less massive) dark halo.

Acknowledgments. I am grateful to Scott Trager and Kyoko Matsushita for providing unpublished results, and to Richard Mushotzky and Ray White for their collaboration on this work. I would also like to thank Patricia Carral and the organizers for a meeting that was outstanding in every way, and to Omar Lopez-Cruz for his guidance.

Discussion

Vladimir Avila Reese: Have you included the gravitational pull of the collapsing baryonic matter on the dark matter halo?

Loewenstein: I've calculated such distortions using the adiabatic approach of Blumenthal et al., but have not incorporated the altered halos into our models – primarily because such an orderly collapse now seems to be a poor approximation to the actual formation of ellipticals. Clearly the effects of baryon evolution on

dark halo structure are important and require further study; however, much depends on the relative timescales of merging, dissipation, and star formation.

Richard Bower: Why do you need to assume a model for the dark matter profile? Why not infer this directly (and uniquely) from the temperature and density profiles? What uncertainty does this introduce?

Loewenstein: Because our goal in this project was to examine the dark matter properties in a statistically meaningful sample, we necessarily include galaxies with only moderately good X-ray data, *i.e* where only a single integrated temperature is derivable and the dark matter profile *cannot* be uniquely determined. For the sake of uniformity we consider only an average temperature for each galaxy in the sample, where the average is taken over an identical *metric* radius of $6R_e$. The total amount of dark matter within this radius is very well determined, but its detailed distribution is not; the NFW function is chosen as a matter of convenience. We hope to follow this general study up with a closer look at individual cases where moderate constraints may be placed on the form of the dark matter distribution, although the crude spatial resolution of X-ray temperature profiles imposes severe limitations.

Paul Eskridge: How much is the $T-\sigma$ relation of Davis and White effected by the hard (non-gaseous) X-ray emission from the relatively faint, low- L_x galaxies?

Loewenstein: Although Davis and White do not include the hard component in their spectral fits to *ROSAT* data, the temperatures they derive are in superb agreement with *ASCA* spectral analysis that *does* include the hard component. I also believe that the trend is primarily driven by gas-rich galaxies that have the smallest temperature uncertainties by virtue of their higher luminosities.

Paul Goudrooij: I think that a significant number of “normal” ellipticals exhibiting X-ray emission from hot gas are dominant members of galaxy groups (small groups of the Huchra/Geller type), so that their low values of β_{spec} may be partly due to the fact that they reside in the center of the group, as well as their own, potential. That is, the hot gas temperature should be compared to the equivalent of the “combined” velocity dispersion of the galaxy plus that of the group in which it resides. Could you comment on this?

Loewenstein: The relevant velocity dispersion for our study that aims to constrain the dark halo relative to optical galaxy properties within the (optically) luminous part of the galaxy is the *central* velocity dispersion, since it is one of the fundamental plane parameters and sets the stellar mass scale. The group velocity dispersion becomes of interest if compared with the outer temperatures of the very extended X-ray halos.

Michael Pahre: There is recent evidence that the scaling of velocity dispersion from central to large radial values may be varying systematically as a function of galaxy luminosity (e.g., Busarello et al. 1997 on mergers of dissipationless systems). How might your results on the luminosity-dependence of dark matter be effected by this property?

Loewenstein: The relative unavailability of velocity dispersion profiles, as well as the sort of complications you raise, motivated our exclusive consideration of central velocity dispersions in this study. For the more detailed study we have

planned, whatever dark halo structure we consider must confront the observations you describe.

Daniel Thomas: Bright ellipticals host α -enhanced stellar populations. If it is mainly these galaxies that enrich the ICM, would you expect a galaxy/ICM asymmetry (Renzini et al. 1993) in the sense that Mg/Fe is underabundant in the ICM? *ASCA* data point towards ratios that are at least not subsolar. What do you think is the best way out of this dilemma?

Loewenstein: Although we have little information on Mg/Fe in the ICM, ratios of other α -elements relative to Fe are supersolar. The *observed* lack of a galaxy/ICM asymmetry implies that one of the assumptions of Renzini et al. (1993) – that star formation in proto-ellipticals has the same mix of SNIa and SNII as our own Galaxy and that the enrichment process in the ICM is prolonged compared to that of the stars – must be abandoned. Also, I believe Renzini et al. probably overestimated the total amount of Fe locked up in stars by a factor of 2–3. More puzzling to me is why the Si/Fe ratio in the hot ISM is \sim solar, in apparent conflict with the stellar Mg/Fe ratio.

References

Arimoto, N., Matsushita, K., Ishimaru, Y., Ohashi, T., & Renzini, A. 1997, ApJ, 477, 128

Brightent, F., & Mathews, W. G. 1997, ApJ, 486, 183

Buote, D. A., & Fabian, A. C. 1998a, MNRAS, 296, 977

Buote, D. A., & Fabian, A. C. 1998b, preprint

Cappellaro, E., Turatto, M., Tsvetkov, D. Yu., Bartunov, O. S., Pollas, C., Evans, R., & Hamuy, M. 1997, A&A, 322, 431

Davies, R. L., Sadler, E. M., & Peletier, R. F. 1993, MNRAS, 262, 650

Davis, D. S., & White, R. E III 1996, ApJ, 470, L35

Fabbiano, G. 1989, ARA&A, 27, 87

Faber, S. M., et al. 1997, AJ, 114, 177

Gibson, B. K., & Matteucci, F. 1997, ApJ, 475, 47

Griffiths, R. E., Casertano, S., Im, M., & Ratnatunga, K. U. 1996, MNRAS, 282, 1159

Hwang, U., Mushotzky, R. F., Loewenstein, M., Markert, T. H., Fukazawa, Y., & Matsumoto, H. 1997, ApJ, 476, 560

Kobulnicky, H. A., & Skillman, E. D. 1997, ApJ, 489, 636

Loewenstein, M., & Mathews, W. G. 1987, ApJ, 319, 614

Loewenstein, M., & Mushotzky, R. F. 1996, ApJ, 466, 695

Loewenstein, M., & White, R. E III 1998, ApJ, submitted

Mac Low, M.-M., & Ferrara, A. 1998, preprint

Mathews, W. G., & Baker, J. 1971, ApJ, 170, 241

Matsushita, K. 1997, Ph.D. thesis, University of Tokyo

Matsushita, K., Makishima, K., Rokutanda, E., Yamasaki, N., & Ohashi, T. 1998, *ApJ*, 488, 125

Matsumoto, H., Koyama, K., Awaki, H., Tsuru, T., Loewenstein, M., & Matsushita, K. 1997, *ApJ*, 482, 133

Matteucci, F., & Gibson, B. K. 1995, *A&A*, 304, 1

Matteucci, F., Ponzone, R., & Gibson, B. K. 1998, *A&A*, in press

Mushotzky, R. F., & Loewenstein, M. 1998, in preparation

Mushotzky, R. F., Loewenstein, M., Awaki, H., Makishima, K., Matsushita, K., & Matsumoto, H. 1994, *ApJ*, 436, L79

Möller, C. S., Fritze-v. Alvensleben, U., & Fricke, K. J. 1997, *A&A*, 317, 676

Navarro, J. F., Frenk, C. S., & White, S. D. 1997, *ApJ*, 490 493

Tantalo, R., Bressan, A., & Chiosi, C. 1998, *A&A*, in press

Worthey, G., Faber, S. M., & Gonzalez, J. J. 1992, *ApJ*, 398, 69